

Volume Fractions of Texture Components of Cubic Materials

J. W. FLOWERS

Research & Technology, Armco Inc., Middletown, Ohio 45043, USA.

(Received October 26, 1982)

A method for obtaining volume fractions in regions about ideal texture components of cubic materials by integration of the orientation distribution function is described. Illustrative examples of the application of the method are given for the primary-recrystallized textures of a 3.15% Si-Fe alloy and several low-carbon steels.

INTRODUCTION

Following the work of Roe (1965, 1966) and Bunge (1965) quantitative texture analysis has been carried out to a significant extent by obtaining a series expansion of the crystallite orientation distribution function (ODF) from the series expansion of measured pole-figure data. In some physical problems the volume fractions of material in regions around selected ideal orientations are of interest. For textures dominated by a few components, the spreads about ideal orientations have been described by Gaussian distributions and integrated ODF values have been obtained using a method proposed by Bunge (1969). However, it is difficult to adequately describe many relatively weak multicomponent textures in this way without using a large number of Gaussian distributions (Morris, 1982).

An alternative method for obtaining volume fractions of texture components for cubic crystals by integration of the ODF is described in the present work. The Euler angle convention used by Roe (1965) is employed, and some properties of this Euler angle space which are relevant to the integration method will be summarized before discussing the method itself.

SOME PROPERTIES OF EULER ANGLE SPACE

The complete ranges of Ψ , θ , and Φ , the Euler angles used by Roe (1965), are $0^\circ \leq \Psi \leq 360^\circ$, $0^\circ \leq \theta \leq 180^\circ$, $0^\circ \leq \Phi \leq 360^\circ$. When each angle is represented along one of three mutually perpendicular axes, the Euler angle space or "Euler volume" is formed. A crystal orientation with Miller indices (hkl) $[uvw]$ is represented at some particular Ψ , θ , Φ location in the Euler volume. Since the (hkl) normal directions are a function of θ and Φ only, they remain unchanged in any constant $-\Psi$ section. For cubic crystal symmetry, a constant $-\Psi$ section may be divided into 48 regions corresponding to the 48 unit spherical triangles on the reference sphere for the standard stereographic projection.

Since the normal directions are fixed by the values of θ and Φ , the Euler

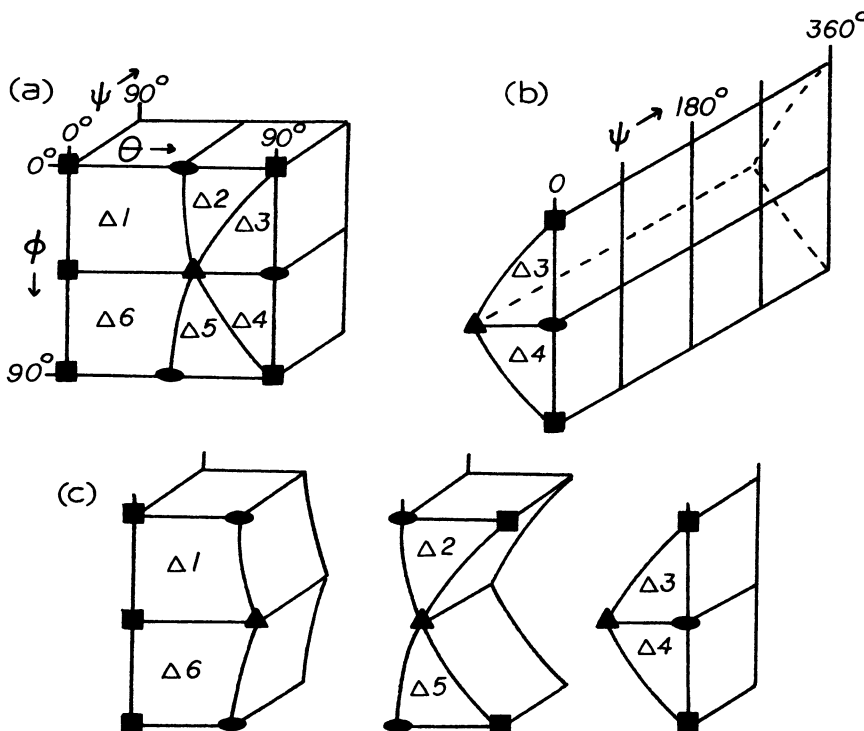


FIGURE 1 Illustrations of several subregions of the Euler volume.

- a) Asymmetric unit;
- b) A cubic subspace;
- c) Division of asymmetric unit into three mathematical subspaces.

volume can be considered as a type of "axis-angle" representation of cubic crystal orientations. For any normal direction, an increase in Ψ corresponds to a counterclockwise (ccw) rotation of a crystal from its initial orientation at $\Psi = 0^\circ$. The ccw rotation is a right-hand screw motion along the positive direction of the rotation axis.

Because of cubic crystal symmetry and possible sample symmetry, it is not necessary to specify ODF values at each point in the full Euler volume to define a texture. The symmetry properties of the ODF in Euler angle space have been discussed by a number of authors (Bunge, 1969; Baker, 1970; Pospiech, 1972; Pospiech *et al.*, 1974; Hansen *et al.*, 1978; Pospiech, 1982). For the common case of cubic crystal symmetry and orthorhombic sample symmetry, texture data are usually presented over the subregion $0^\circ \leq \Psi \leq 90^\circ$, $0^\circ \leq \theta \leq 90^\circ$, $0^\circ \leq \Phi \leq 90^\circ$. This subregion, called the "asymmetric unit" (Baker, 1970) or the " $90^\circ \times 90^\circ \times 90^\circ$ volume", has a projection on a constant $-\Psi$ plane equal to that of 6 stereographic triangles (Figure 1a). This subregion contains at least 3 representations of a general $\{hkl\} \langle uvw \rangle$ orientation, so this subregion contains redundant information.

TABLE I
Relations Among the Four General $\{\text{HKL}\} \langle \text{UVW} \rangle$ Orientations in a Cubic Subspace

Orientation	Relation to I	Matrix Representation	Relative Euler Angles
I. $(\text{HKL})[\text{UVW}]$ Δ_3	Identity	$[T]$	Ψ, θ, Φ
II. $(\text{HKL})[\bar{U}\bar{V}\bar{W}]$ Δ_3	Obtained by 180° rotation about crystal vector parallel to space-fixed z.	$[T'] = [T][Pz]$	$\Psi' = 180^\circ + \Psi$ $\theta' = \theta$ $\Phi' = \Phi$
III. $(\bar{K}\bar{H}\bar{L})[\bar{V}\bar{U}\bar{W}]$ Δ_4	Obtained by 180° rotation about crystal vector parallel to space-fixed x.	$[T'] = [c][T][Px]$	$\Psi' = 180^\circ - \Psi$ $\theta' = \theta$ $\Phi' = 90^\circ - \Phi$
IV. $(\bar{K}\bar{H}\bar{L})[\bar{V}\bar{U}\bar{W}]$ Δ_4	Obtained by 180° rotation about crystal vector parallel to space-fixed y.	$[T'] = [c][T][Py]$	$\Psi' = 360^\circ - \Psi$ $\theta' = \theta$ $\Phi' = 90^\circ - \Phi$

$$[T] = \text{Roe's T Matrix}, [c] = \begin{bmatrix} 0 & 1 & 0 \\ 1 & 0 & 0 \\ 0 & 0 & -1 \end{bmatrix}$$

Roe (1965); Eq. (4)

$$[Px] = \begin{bmatrix} 1 & 0 & 0 \\ 0 & -1 & 0 \\ 0 & 0 & -1 \end{bmatrix}, [Py] = \begin{bmatrix} -1 & 0 & 0 \\ 0 & 1 & 0 \\ 0 & 0 & -1 \end{bmatrix}, [Pz] = \begin{bmatrix} -1 & 0 & 0 \\ 0 & -1 & 0 \\ 0 & 0 & 1 \end{bmatrix}$$

In order to define integrals within the Euler volume which can be interpreted as volume fractions, it is first necessary to define the regions of the Euler volume which contain each general asymmetric cubic orientation once and only once. To do this, we note that a general $\{hkl\} \langle uvw \rangle$ set of cubic orientations has 96 members when all crystallographically permissible permutations of the letters and sign changes are considered. However, the 96 members are not all distinct in a physical sense. The 96 orientations may be separated into 4 main orientations from each of which 24 members can be generated by application of the 24 cubic symmetry operations. Since the application of a cubic symmetry operation amounts only to a relabeling of the original configuration, it follows that at most only the 4 main orientations of the set of 96 members can be physically distinct. These 4 main orientations may be listed as follows: I— $(HKL) [UVW]$; II— $(HKL) [\overline{U}\overline{V}\overline{W}]$; III— $(\overline{H}\overline{K}\overline{L}) [\overline{U}\overline{V}\overline{W}]$; IV— $(\overline{H}\overline{K}\overline{L}) [UVW]$.

As indicated in Table I for the 4 main orientations which lie in subregions of the Euler volume bounded by stereographic triangles $\Delta 3$ and $\Delta 4$ in Figure 1a, orientations II, III, and IV are related to orientation I by 180° ccw rotations about crystal vectors parallel to the space-fixed z, x, and y directions, respectively. Since in general these crystal vectors are not $\langle 100 \rangle$ or $\langle 110 \rangle$ axes, orientations I, II, III, and IV are physically distinct in general and must be included in a subregion including all possible cubic crystal orientations. The relative Euler angles for these 4 orientations in $\Delta 3$ and $\Delta 4$ may be obtained by equating the matrix equations in Table I element by element with the results also shown in Table I. Since these results hold for all asymmetric orientations in the subregion of the Euler volume bounded by these two triangles, it follows that a subregion bounded by these two triangles and extending from $\Psi = 0^\circ$ to $\Psi = 360^\circ$ will be required to include all possible cubic orientations. This subregion will be called a cubic subspace (CSS) and is illustrated in Figure 1b. Twenty-four CSS's are contained within the full Euler volume.

The cubic orientations within a CSS can be regarded as being generated by ccw rotations about each of the normal directions in two stereographic triangles with the normals in one triangle having the negative sense of the normals in the other triangle. There are a number of equivalent ways of forming CSS's within the Euler volume as shown in prior work (Pospiech, 1972; Hansen *et al.*, 1978; Pospiech, 1982).

When orthorhombic sample symmetry exists as well as cubic crystal symmetry, a subregion smaller than a CSS is sufficient for the representation of all of the ODF values for a given texture (Pospiech, 1972; Hansen *et al.*, 1978; Pospiech, 1982). With orthorhombic sample symmetry the general orientations I, II, III, and IV in Table I all have identical ODF values. This leads to the repetition pattern of ODF values within a CSS given in Figure 2.

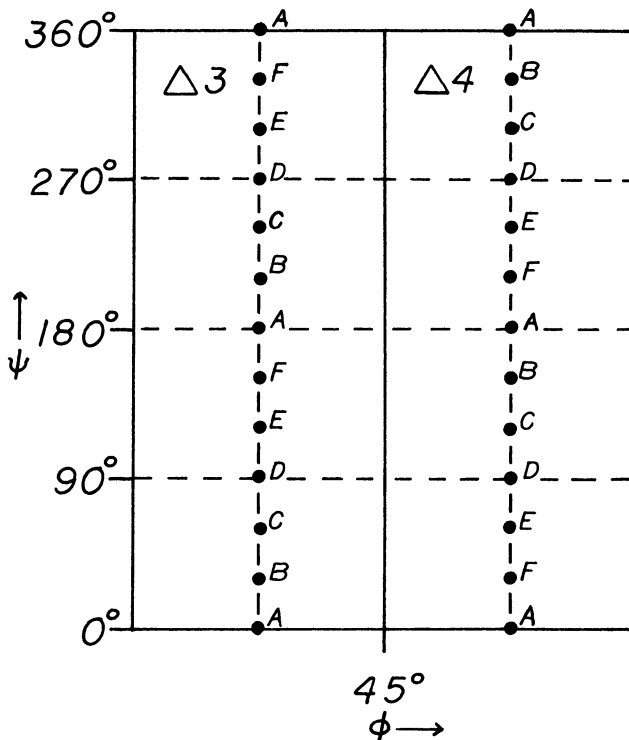


FIGURE 2 Repetition pattern for ODF values on a constant $-\theta$ section of a cubic subspace with orthorhombic sample symmetry.

This illustration shows that a complete set of ODF values can be represented in a subregion equal to 1/4 of a CSS; this subregion will be called a mathematical subspace (MSS). There are a number of equivalent ways of forming MSS's; the division of the $90^\circ \times 90^\circ \times 90^\circ$ asymmetric unit into 3 MSS's is shown in Figure 1c.

If both cubic crystal symmetry and orthorhombic sample symmetry are present, a complete set of ODF data can be presented in a compact form, for example, by means of a set of constant- Ψ sections for one MSS. A representation in this form is similar to that used by Williams (1968) for his biaxial pole figures.

CALCULATION OF VOLUME FRACTIONS OF TEXTURE COMPONENTS

Since the ODF, $w(\Psi, \theta, \Phi)$, gives the probability density for the occurrence

of crystals within an elementary volume of Euler angle space (Roe, 1965), its integral over a volume element can be interpreted as the volume fraction of crystals within the orientation range of the element if the integral is properly normalized. The ODF has been defined so that its integral over the Euler volume is unity (Roe, 1965; Eq. 2):

$$\int_0^{2\pi} \int_0^{2\pi} \int_{-1}^1 w(\cos\theta, \psi, \phi) d(\cos\theta) d\psi d\phi = 1 \quad (1)$$

or in abbreviated form as:

$$\int_V w dV = 1 \quad (2)$$

However, in most applications the ODF is expressed in times random (xR) units, w_{xR} , so that the value of the ODF is unity everywhere for a random specimen. In this case:

$$(1/8\pi^2) \int_V w_{xR} dV = 1, \text{ and } w_{xR} = 8\pi^2 w \quad (3)$$

Since a CSS is 1/24 of the total Euler volume, we may define an ODF normalized over a CSS, w_c , as follows:

$$\int_{\text{CSS}} w_c dV = 1, \text{ where } w_c = 24w = (3/\pi^2)w_{xR} \quad (4)$$

The volume fraction, f , over a volume element ΔV within a CSS may then be expressed by:

$$f = \int_{\Delta V} w_c dV = 24 \int_{\Delta V} w dV = (3/\pi^2) \int_{\Delta V} w_{xR} dV \quad (5)$$

In applications, it may be simpler to estimate the average value of w_{xR} , \bar{w}_{xR} , over a volume element ΔV , and calculate f from:

$$f = (3/\pi^2) \bar{w}_{xR} \Delta V \quad (6)$$

In the present work cylindrical volume elements about ideal orientations were used for integration. These elements are formed from circles of radius r drawn about the orientations of interest on a constant $-\Psi$ plane which

are projected in the plus and minus Ψ directions to form cylinders. The elements contain orientations with normals within r^0 of the ideal orientations's normal and all orientations generated from these by rotations of $\pm \Delta\Psi$ about each normal in the circle of radius r . As long as the radii of the circles and the values of $\Delta\Psi$ are kept constant, elements of this type have the same angular volume about each orientation.

Because of the geometric shape of a CSS, cylindrical volume elements for an ideal orientation of high symmetry which occurs multiple times on the bounding surfaces of a CSS must be formed by combining partial elements at each location of the ideal orientation. Examples for several ideal orienta-

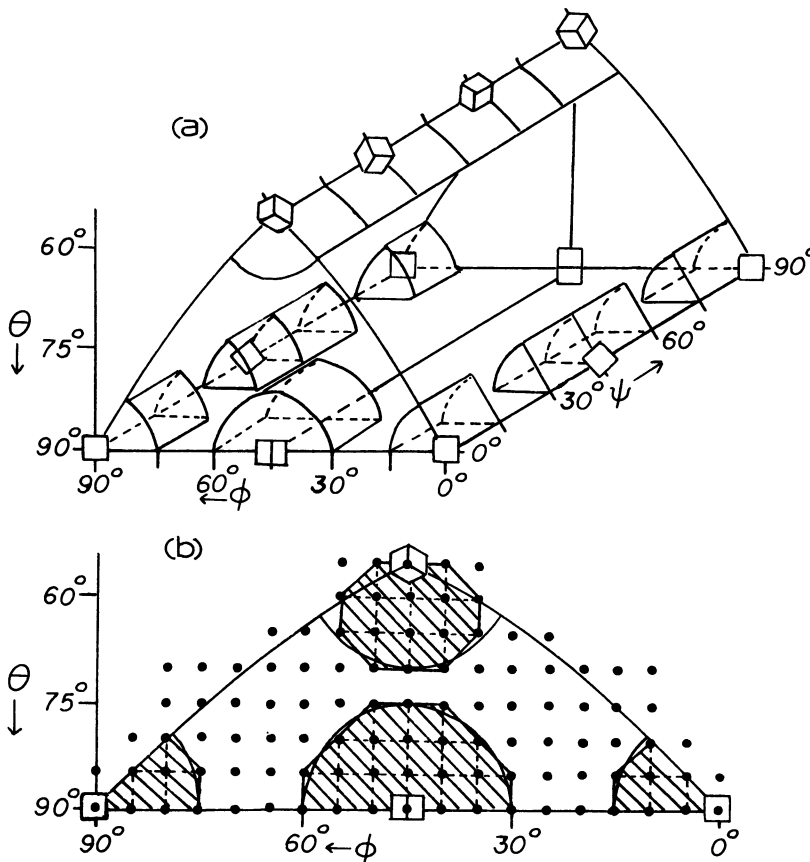


FIGURE 3

- a) Illustration of cylindrical volume elements formed around selected ideal orientations;
- b) Illustration of procedure for approximate numerical integration.

tions in the CSS shown in Figure 1b are given in Figure 3a for values of r and $\Delta\Psi$ of 15°. An element for a {110} <001> orientation, for example, is formed by adding together the quarter-element at $\Psi = 0^\circ$, the two quarter-elements at $\Psi = 180^\circ$, and the quarter-element at $\Psi = 360^\circ$. Similarly, volume elements for each of the 2 twin-related orientations of the {111} <112> or {111} <011> types are formed by adding 1/6 elements and elements for orientations of the {100} <001> or {100} <011> types are formed by adding 1/16 elements. When orthorhombic sample symmetry exists, computation may be limited to an MSS because of the mathematical symmetry illustrated in Figure 2.

Since analytical integration over irregularly-shaped regions is difficult, an approximate numerical integration method was used to obtain the results to be discussed in this work. Values of the ODF in xR units were obtained at 5° increments of Ψ , θ , and Φ . Each 5°-cube in the asymmetric unit of the Euler volume was weighted by the average ODF value of its corner points, and the volume elements of integration were approximated by sets of cubes and half-cubes as illustrated in Figure 3b. The average ODF value was calculated for each approximated volume element, and the volume fraction for each element was computed by using Eq. (6).

ILLUSTRATIVE EXAMPLES

Data for 2 specimens will be given to illustrate the application of the integration method discussed above. Specimen P-3 was prepared from primary-recrystallized sheets of 3.15% Si-Fe representing an intermediate stage in the production of "grain-oriented" Si-Fe by selective secondary growth of primary grains with the {110} <001> orientation. These sheets were processed as discussed previously (Flowers and Heckler, 1976) including two stages of cold rolling with reductions of 67% and 59% with an intermediate anneal. After the second cold rolling, the sheets were annealed at 830° for 2 min. to effect decarburization and primary recrystallization. A composite X-ray specimen was used for the determination of (110), (002), and (112) pole figures with an Enraf-Nonius CAD-4 diffractometer, and ODF values were calculated to 16th order, using even- l terms only, by a procedure similar to that of Morris and Heckler, 1968.

The second specimen, P-25, was prepared from sheets of a fully-processed, Cb-treated, "interstitial-free" steel used in deep-drawing applications. The chemistry, processing, and partial ODF data for this material were given by Hook *et al.* (1975) (their Steel 25). The ODF data were also determined on a composite sample to 16th order, using even- l terms only.

Since it has been shown that the omission of odd- l terms in ODF calcula-

tions introduces errors of uncertain magnitude in general (Matthies, 1979; Lücke *et al.*, 1981), the ODF data for the two specimens must be regarded as approximate. Because orthorhombic sample symmetry existed for both specimens, complete ODF data for them can be presented concisely using constant $-\Psi$ sections through the MMS formed by the triangular subregions $\Delta 3$ and $\Delta 4$ in Figure 1c. The sections for specimens P-3 and P-25 are given in Figures 4 and 5, respectively. Since the element of spherical surface area in $\sin\theta d\theta d\Phi$, the θ -scale in Figures 4 and 5 is actually plotted as $\cos\theta$ to make the constant $-\Psi$ sections area-true. The locations of some ideal orientations and some of the normal directions which are constant in each section are given on the figures. More detailed indexing may be accomplished, for example, by using the charts published by Davies *et al.*, 1971.

The constant $-\Psi$ sections for the 3.15% Si-Fe specimen P-3 in Figure 4 show that there are two relatively intense bands of orientations in a generally weak overall texture. The first is centered about the $\theta = 90^\circ$ line on the $\Psi = 0^\circ$

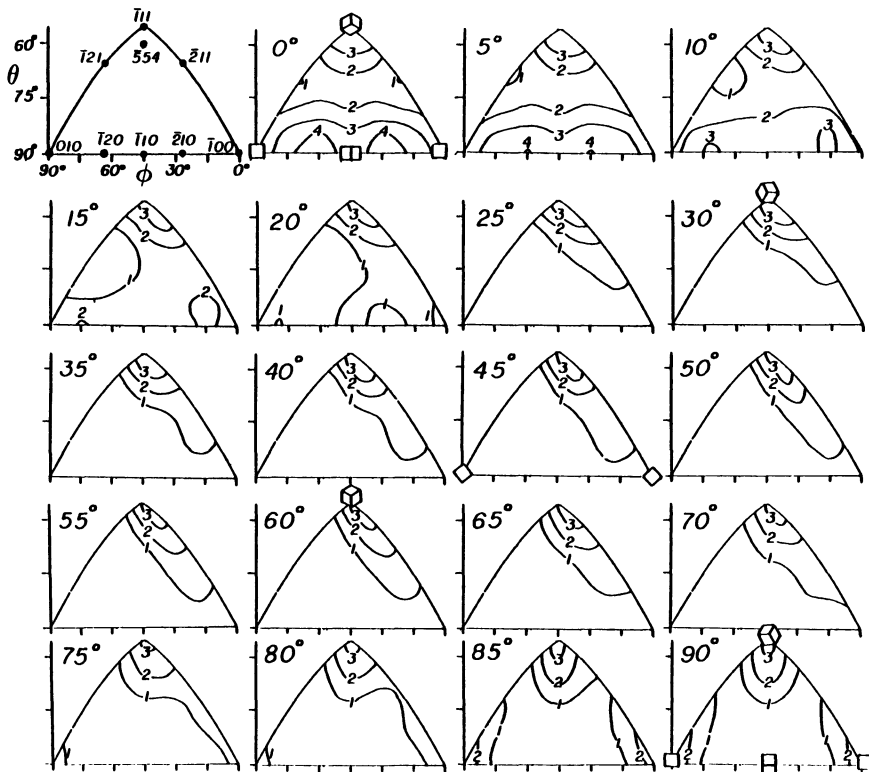


FIGURE 4 Constant $-\Psi$ ODF sections for specimen P-3.

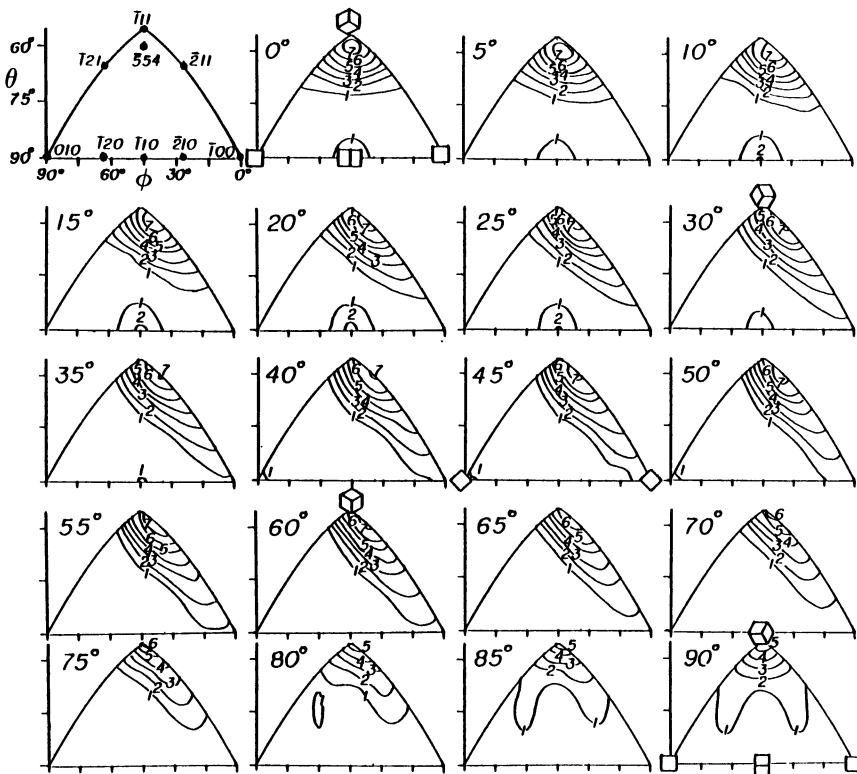


FIGURE 5 Constant $-\Psi$ ODF sections for specimen P-25.

section and includes orientations at or near the {HKO} $\langle 001 \rangle$ type. The second band of orientations is centered approximately about the $[\bar{1}\bar{1}\bar{1}]$ normal and remains roughly constant over a range of Ψ from 0° to 90° . These general features have been discussed previously (Morris and Heckler, 1968; Flowers and Heckler, 1976). In contrast to the prior work, however, where the ODF maximum occurred at the ideal $\{110\} \langle 001 \rangle$ orientation, the maxima for specimen P-3 occurred near the positions for the ideal doublet- $\{210\} \langle 001 \rangle$ orientations ($\Psi = 0^\circ$ section) and had values slightly above $4 \times R$.

Integrated ODF data for volume elements centered about selected ideal orientations for specimen P-3 are given in Table II. The cylindrical element discussed above was used with values of 15° for r and $\Delta\Psi$. An element of this size comprises 3.4% of the total angular volume of a CSS. The amounts of the orientations near $\{110\} \langle 001 \rangle$ in this primary texture are of particular interest, since grains with these orientations grow selectively during subsequent processing and consume the balance of the material. As shown in

TABLE II
Integrated ODF Values for $\pm 15^\circ$ Cylindrical Volume Elements Centered about Selected Ideal Orientations.

Ideal Orientation	Specimen P-3		Specimen P-25	
	Ideal ODF Value	Volume % by $\pm 15^\circ$ Integrations	Ideal ODF Value	Volume % by $\pm 15^\circ$ Integrations
(111)[112]	3.2 xR	7% (2.2 xR)	6.8 xR	17% (4.9 xR)
(111)[211]	3.2 xR	7% (2.2 xR)	6.8 xR	17% (4.9 xR)
(111)[011]	3.5 xR	7% (2.2 xR)	5.3 xR	11% (3.1 xR)
(111)[110]	3.5 xR	7% (2.2 xR)	5.3 xR	11% (3.1 xR)
(100)[011]	0.5 xR	2% (0.5 xR)	1.1 xR	2.5% (0.7 xR)
(110)[001]	3.5 xR	8% (2.4 xR)	1.7 xR	1.7% (0.5 xR)
(100)[001]	2.5 xR	6% (1.9 xR)	0.7 xR	0.5% (0.1 xR)

Table II, grains in the $\pm 15^\circ$ element about ideal {110} <001> amounted to approximately 8% of the volume of this specimen. Volume elements about {111} <112> and {111} <011> orientations had volume percentages of approximately 7% each, so the combined amount of the 2 twin-related members of both types was approximately 28% of the specimen by volume. Volume fractions about {100} <001> and {100} <011> orientations were approximately 6% and 2%, respectively. These integrated ODF data emphasize the relatively weak nature of the primary texture of this important transformer core material.

The constant $-\Psi$ sections for P-25, the deep-drawing steel specimen, show (Figure 5) that a dominant band of orientations with maximum ODF values of over 7 xR is centered approximately in the region between the [111] and [211] normals. This band maintains ODF values of at least 5 xR over the complete range of Ψ from 0° to 90° . Outside this band only relatively small regions have ODF values as high as 2 xR. The tendency of this specimen to have a strong fiber texture about the [111] sheet normal is considered to be a major factor in its very good deep-drawability (Hook *et al.*, 1975).

Integrated ODF values about selected ideal orientations for specimen P-25 using the $\pm 15^\circ$ volume element are listed in Table II. Elements about each of the 2 twin-related {111} <112> components have volume fractions of approximately 17% while elements about each of the 2 twin-related {111} <011> components have volume fractions of 11%. In total, grains with orientations in these 4 elements represent over half the specimen by volume. None of the elements about the {100} <011>, {110} <001>, or {100} <001> orientations contain volume fractions as high as 3%. Other aspects of the texture of this specimen in relation to its deep-drawability have been discussed earlier (Hook *et al.*, 1975).

For some physical problems only the amounts of material with normal directions close to some ideal axes are of interest. These amounts may be

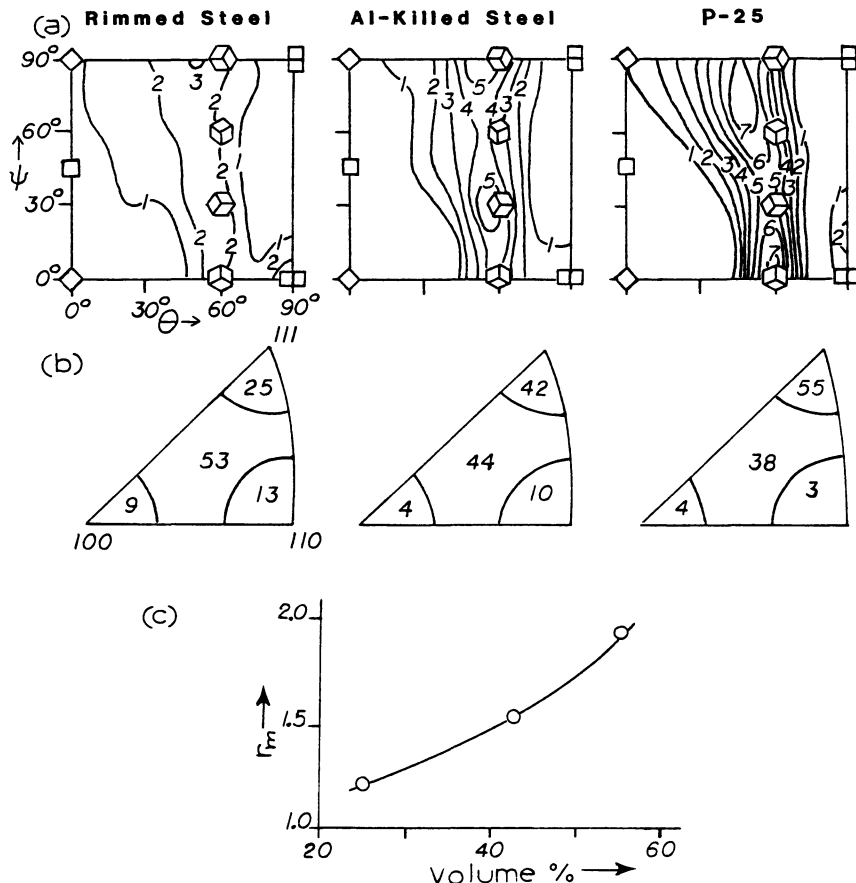


FIGURE 6 Texture data for low-carbon steels.

- ODF sections at $\Phi = 45^\circ$;
- Volume percentages of material with plane normals in indicated regions of stereographic triangle;
- Average plastic strain ratio, r_m , vs. volume percentage of material with normals within 15° of $\langle 111 \rangle$.

obtained by ODF integrations using an extension of the method used for integration about ideal orientations. For example, the volume fractions with normals within 15° of the $\langle 100 \rangle$, $\langle 110 \rangle$, and $\langle 111 \rangle$ axes may be obtained by numerical integration over the volumes formed by projecting the areas shown as cross-hatched regions in Figure 3b over the range $0^\circ \leq \Psi \leq 360^\circ$. The results may be displayed in a single stereographic triangle and represent information similar to that shown on conventional normal-direction inverse

pole-figures, but the results are expressed on a direct volume fraction basis.

An application of this method is illustrated in Figure 6 for 3 low-carbon steels. Sections of the ODF at $\Phi = 45^\circ$ published previously by Heckler and Granzow (1970) are given in Figure 6a for a rimmed steel and an Al-killed steel both processed through box-annealing to 737°C along with a $\Phi = 45^\circ$ section for P-25 (Hook *et al.*, 1975). The volume percentages of material with normals within 15° of the $\langle 100 \rangle$, $\langle 110 \rangle$, and $\langle 111 \rangle$ axes are plotted for these steels in stereographic triangles in Figure 6b. It is evident that the volume percentage with normals within 15° of $\langle 111 \rangle$ increases significantly for the Al-killed steel compared to the rimmed steel, and increases still further for P-25. The deep-drawability of a steel is improved when its average plastic strain ratio, r_m , is increased, and higher r_m values are obtained when the amount of material with normals near $\langle 111 \rangle$ is increased (Burns and Heyer, 1958). The r_m values obtained from the original papers for the particular steels in Figure 6 are plotted vs. the volume percentages of material with normals within 15° of $\langle 111 \rangle$ in Figure 6c. It is evident that a good correlation exists.

DISCUSSION

The method described above for obtaining volume fraction data by integration of the ODF may be particularly well-suited for application to materials with relatively weak multicomponent textures. Many materials of industrial importance have textures of this general type. Numerical integration may be particularly useful when the orientation regions of interest in a physical problem have irregular geometric shapes in the Euler volume.

Acknowledgement

Helpful discussions with P. R. Morris are gratefully acknowledged.

References

- Baker, D. W. *Advances in X-Ray Analysis* **13**, 435 (1970).
- Bunge, H. J. *Z. Metallkde.* **56**, 872 (1965).
- Bunge, H. J. *Mathematische Methoden der Texturanalyse*. Akademie-Verlag, Berlin (1969).
- Burns, R. S. and Heyer, R. H. *Sheet Metal Ind.* **35**, 261 (1958).
- Davies, G. J., Goodwill, D. J. and Kallend, J. S. *J. Appl. Cryst.* **4**, 67 (1971).
- Flowers, J. W. and Heckler, A. J. *IEEE Trans. on Magnetics MAG-14*, 846 (1976).
- Hansen, J., Pospiech, J. and Lücke, K. *Tables for Texture Analysis of Cubic Crystals*. Springer-Verlag, Berlin (1978).
- Heckler, A. J. and Granzow, W. G. *Met. Trans.* **1**, 2089 (1970).

- Hook, R. E., Heckler, A. J. and Elias, J. A. *Met. Trans.* **6A**, 1683 (1975).
Lücke, K., Pospiech, J., Virnich, K. H. and Jura, J. *Acta Metall.* **29**, 167 (1981).
Matthies, S. *Phys. Stat. Sol. (b)* **92**, K135 (1979).
Morris, P. R. and Heckler, A. J. *Advances in X-Ray Analysis* **11**, 454 (1968).
Morris, P. R. Submitted to *Textures and Microstructures* (1982).
Pospiech, J. *Kristall u. Technik* **7**, 1057 (1972).
Pospiech, J., Gnatek, A. and Fichter, K. *Kristall u. Technik* **9**, 729 (1974).
Pospiech, J. "Symmetry analysis in the space of Euler angles". In: *Quantitative Texture Analysis*. D. G. M. Metallurgy Information, New York (1982).
Roe, R. J. *J. Appl. Phys.* **36**, 2024 (1965).
Roe, R. J. *J. Appl. Phys.* **37**, 2069 (1966).
Williams, R. O. *Trans. AIME* **242**, 105 (1968).